IEEE Access
Multidisciplinary | Rapid Review | Open Access Journal

Received March 2, 2021, accepted March 14, 2021, date of publication March 19, 2021, date of current version March 30, 2021.

Digital Object Identifier 10.1109/ACCESS.2021.3067360

Muscle Activation Visualization System Using Adaptive Assessment and Forces-EMG Mapping

XUYANG WEI, YAN CHEN, XUEYU JIA, YITING CHEN, AND LONGHAN XIE, (Member, IEEE)
Shien-Ming Wu School of Intelligent Engineering, South China University of Technology, Guangzhou 510640, China

Corresponding author: Longhan Xie (melhxie@scut.edu.cn)

This work was supported in part by the National Natural Science Foundation of China under Grant 52075177, in part by the Joint Fund of the Ministry of Education for Equipment Pre-Research under Grant 6141A02033124, in part by the Research Foundation of Guangdong Province under Grant 2019A050505001 and Grant 2018KZDXM002, in part by the Guangzhou Research Foundation under Grant 202002030324 and Grant 201903010028, in part by the Zhongshan Research Foundation under Grant 2020B2020, and in part by the Shenzhen Institute of Artificial Intelligence and Robotics for Society under Grant AC01202005011.

ABSTRACT VR-based serious games are obtained without details about real-time guide and feedback in the rehabilitation after stroke, leading to undesirable recovery outcomes. This study investigated the feasibility of real-time visualization in muscle state feedback by sEMG. Then we explored the application in movement guide and diagnosis. We provided a force-sEMG mapping approach based on body weight to visualize the implicit bioinformation. And 10 healthy subjects participated in an experiment that the K-means cluster algorithm and the support vector regression are employed to filter the unexpected data and adjust the visualization parameter for each subject dynamically. The verification experiment demonstrates that force and sEMG can be mapped as a data pair by support vector regression and normalized by the low-cost calibration in 6-8 times reparative actions. We define the predictive accuracy as the ratio of the predicted to the practical tasks. And mean absolute value is the most suitable index to compete for most data scales which can provide a predictive accuracy of 89.84% $\pm$ 5.28% in biceps and 84.26% $\pm$ 6.44% in triceps. We present the motivation improvement for patients and supervision in online and offline application scenarios for therapists. This system can be applied in precision and telemedicine to improve the efficacy of rehabilitation by objective data and intuitive expression through visualization.

INDEX TERMS K-means cluster, rehabilitation, surface electromyography, stroke, SVR, visualization.

I. INTRODUCTION

VR-based serious games are extensively implemented in the rehabilitation of stroke. The virtual environments (VEs) and attractive tasks are significant causes for improving activities of daily living after stroke. The alternative for traditional tedious tasks is apparent, as VEs make survivors finish intensive task-oriented training with negative emotion decreasing [1].

However, current researches focus on the macroscopic bioinformation like the transform of the affected limb. Though complementary motion tasks in VEs improve the motivation of long-term training [2], [3], only a few VEs pay attention to the bioinformation under the skin, such as the sEMG and biomechanics. In developing countries like China, VR-based remote diagnosis is becoming a solution to make up for the shortage of rehabilitation resources in villages [4]. Therapists supervise the rehabilitation process behind the screen with the score gained by patients during the serious game [5], [6]. Instead of comprehensive analysis and presentation, it is only the result of periodic rehabilitation training. Based on this indicator, both patients and therapists are blind to the cause behind rehabilitation performance without the acceptable details about bioinformation [7], [8]. Similarly, the scale and the derived method of motor performance evaluation only reflect the rehabilitation results. A large number of clinical trials have been conducted to determine the standard of assessing the recovery status of patients. Nonetheless, people always ignore the inaccurate patients' feedback on their conditions caused by factors including decreased language expression ability and depression in the assessment process. At all events, bioinformation is inadequate for therapists when the subjective perception of the patient is the only feedback to adjust the plan of rehabilitation.

Therefore, two approaches for stroke rehabilitation diagnosis have been employed to stay objective: the

The associate editor coordinating the review of this manuscript and approving it for publication was Wenbing Zhao.

assessment scales and the automatic assessment algorithm. Jennifer K Harrison and Iacono, Laura A. reviewed more than eight kinds of neurological assessment scales. Iacono, Laura A pointed out that different patients need the assessment scales fitted them. However, the experience of the therapist affects choose of scales seriously [9], [10]. Taylor-Rowan even focused on the exemplars of assessments that describe impairment, activity, participation, and quality of life [11]. Their study expanded the scope of assessment scales. In 2019, Krumlinde paid close attention to the bimanual performance for adults after stroke and designed the observation-based valid functional measure of bimanual performance [12]. In the latest research, Ho, Lily set up the Chinese version of the Fatigue Assessment Scale to assessing fatigue [13]. Furthermore, they also determined the relationship between fatigue and the psychological state. In 2015, Li, Hsin-Ta found the problem of carelessness in the traditional assessment, and develop a stroke rehabilitation assessment system by using inertial measurement units [14]. The system had the potential to overcome some shortcomings of traditional assessment methods and indicates rehab performance correctly. In the latest study, Oubre and his colleagues tried to draw an unsupervised clustering algorithm and a supervised regression model into Fugl-Meyer Assessment scores based on movement features [15]. This work improved the speed of detection. Rahman and his team designed the robot-based assessment modules for breaking through the limit of the traditional assessment scales. Moreover, they found that the kinematic variables extracted from assessment modules can be used as a standard for assessing stroke patients [16]. In 2018, Chang Hong, and his team design mobile phone application-based scales to make the self-assessment of acute stroke patients accurate, economic, and convenient [17].

Although the accuracy and efficiency have been emphasized with attention given to the assessment in most studies of assessment scales, the approach of bioinformation show is unsatisfactory. The visualization of bioinformation will make up for the shortage of medical resources with the development of wearable devices and communication technology. Bioinformation visualization technology, as a fusion of computer graphics and bioinformatics, establish the mapping relationship between the data from sensors and VEs. It makes patients understand their status and help therapists diagnose accurately [18]. Motion information assists patients participate the human-computer interaction tasks and can be stored as analytical data due to motion capture technology [19], [20]. Both patients and therapists get more direct-viewing effects compared with traditional methods seemingly. Nevertheless, the therapists have difficulty in evaluating the quality of movement comprehensively because the motion bioinformation which may come from movement related to compensatory behaviors.

To integrate the assessment method, surface electromyography (sEMG) is skillfully implemented in rehabilitation after stroke and control of artificial limb owing to its non-invasively and harmless feature [21]. Hence, it is necessary to integrate the time or frequency domain sEMG graph into the accessible style. In previous work, people realize the activation patterns of muscles are under a similar mapping relationship by processed through different algorithms [22]. The similarity means that the degree of muscle activation (DMA) can be measured and shown. What we require it's not only to show the objects' past sEMG through 3D-models in VEs [18], but we also need a real-time display and meaningful interactions. Such a data-driven-based real-time DMA visualization architecture is an effective supplement for traditional rehabilitation and remote diagnosis. People quantize the degree as a ratio of signal at a particular time to peek at the stage. After processing the sEMG signal, the DMA is displayed on the screen for both patients and therapists. So that therapists can evaluation the rehabilitation conditions quantitatively instead of empirically. The traditional rehabilitation diagnosis is based on the movement information of patients, which is superficial for therapists. To study the root cause of the abnormal muscle activities, therapists need to observe the coordination and activation state of muscles under the skin intuitively, instead of the hysteresis which leads to communication barriers during the consultation [23]. To our investigation, no studies have set up a real-time visualization model for the DMA based on sEMG.

The purpose of this study is to verify the mapping relationship between muscle force and sEMG features and explore an approach to visualize the DMA. Our contributions are as follows:

1) Real-time sEMG signal normalization method: we explored the relationship between weight and MVC, the compensation coefficient in the process of prediction, and the predictive effect of various sEMG indicators.

2) Based on the idea of the K-means cluster algorithm, we designed a real-time sEMG signal normalization method that provides the interface of concretizing abstract sEMG.

3) Visualization and bioinformation database: we developed a prototype of the supervision system for stroke rehabilitation. This system is multi-platform and low-cost, which can casualize the visualization of muscle condition to both therapists and patients. Bioinformation is stored into a certain database on the cloud server as an e-medical record which can be extracted by multiple terminals with live or playback models all the time.

II. MATERIALS AND METHODS

A. SYSTEM IMPLEMENTATION

As shown in Figure 1(A), the main component of the measurement hardware is the USB5936 (Zijin Electronic Studio, China), a wired sEMG collector. The sEMG data measured in advance are processed and stored in a database on PC. At the same time, the measurement platform helps calibration with digital display dynamometer and hand shank. In the end, the screen shows all the essential details for both therapists and patients. In Figure 1(B), the musculoskeletal models in colorful represent the DMA mapping to the chromatographic column sidebar.

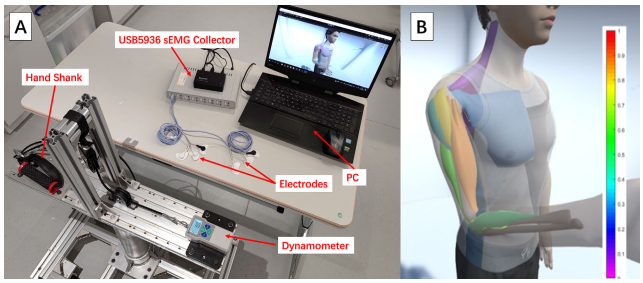

FIGURE 1. Implementation of DMA visualization system. (A) The necessary components. (B) The UI of DMA visualization, slider color bar helps to check the DMA.

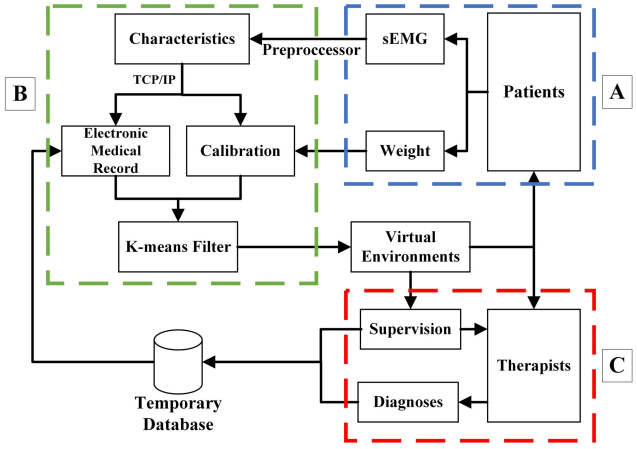

FIGURE 2. Data flow can be divided into three parts: (A) Collection; (B) Processing; (C) Application.

TABLE 1. Information on male subjects with right hand.

Participant	Age	Weight(kg)
P1	26	56.0
P2	23	61.1
P3	25	63.0
P4	23	55.5
P5	23	59.9
P6	24	74.0
P7	26	81.0
P8	23	57.7
P9	21	58.0
P10	24	68.0

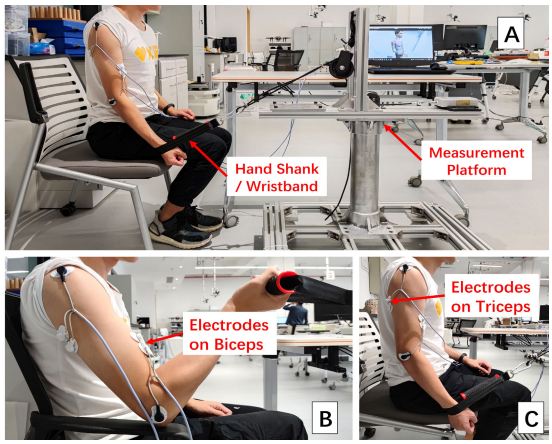

FIGURE 3. Measurement platform (A) and experiment in elbow (B) flexor and (C) extensor show.

Figure 2 shows the data flow chart. sEMG data will flow in multiple directions throughout the system and eventually merge into a loop, forming effective bioinformatic feedback that helps therapists and patients make necessary adjustments to the rehabilitation process.

B. PARTICIPANTS

We recruit 10 subjects (N = 10, age 23.8 ± 1.5 years, body mass 63.4 ± 8.4 kg, all-male and all right-handed) to participate in the verification test. All the subjects are male, without any tissue damage or over fatigue. Table 1 presents an overview of the data used in this paper. MVC is assessed by the subjects' body weight. There is a significant regression relationship between the strength of elbow muscles and body weight [26].

Elbow torque and body weight was shown to be correlated in a logarithmic manner when the upper limb muscles contracted isometrically in a given position. Therefore, we deduced (11) according to this conclusion, and introduced the parameter C_{com} to correct for differences between different races in the verification experiment. In our study, the aim is not to see the actual influence of the subject's weight on the experimental results. The experiment of the prediction is to find the correction of the coefficients in the previous study. And participants were recruited to test the feasibility of visualizing EMG signals through a practical test.

C. EXPERIMENTAL PROCEDURE

The experiment is conducted on a force measuring platform as shown in Figure 3(A). Aluminum profiles as the base for extendable installation provide a low-cost option for the selection of accessories. The rope runs through a pulley block, with one end connected to a digital display dynamometer that can accurately indicate the number, and the other end to a handle for the subject to hold. In the pulley block, two fixed pulleys are set on the bottom of the base and girder respectively to ensure both result accuracy and direction freedom in the measurement process.

Participants firstly stood on the electronic scale to measure body weight. Then, the body weight was input to the UI system (see Figure 1(A)) to assess the MVC of subjects by (1) and (2). Then, the skin over target muscles was cleaned with 70% alcohol and attached to 1cm diameter electrodes without hydrophilic electrolyte. We followed the localization, orientation for setting the electrodes suggested by recommendations of sEMG [24], [25]. The reference electrode was placed on the elbows of participants.

Every participant performed two experiments including biceps and triceps so that we can collect how such a visual system works in both flexor and extensor muscles. Each experiment consisted of two sessions, including the control group which is performed by the actual MVC, and the experimental group which is performed by the predicted MVC. In the experimental group, participants were asked to make the force between 0 and the actual MVC with isometric contraction in 9 times. Every participant hereto gets a group of sample points including 1 for the quiescent condition, 9 for random force, and 1 for the actual MVC. In the subsequent processing, the groups of random sample points are training sets, and the actual MVC sample points are the test sets.

In the biceps verification test of mapping relationship, we firstly arranged subjects to sit on the adjustable armchair, modifying the appropriate height to relax as shown in Figure 3(B). Then, they flexed the elbow as hard as possible to record the actual MVC and the original sEMG signal. In the next step, subjects made them elbow of dominant hand on the armrest, and hold the handle of the measurement platform to get a group of force-sEMG key-value pairs which begins with the quiescent condition randomly. All the duration of the test is 3 seconds to control the variable and ensure the reliability of the result. We took the advantage of such key-value pairs to get a regression curve in which the predicted MVC can cut off an sEMG value for the normalization of DMA visualization.

In terms of the triceps, similar steps are set and subjects just need to change their performance style by drooping their arm naturally and pressing the wristband with a wrist arch. In Figure 3(C), experimental actions are demonstrated.

1) DYNAMOMETRY

MVC is a difficult measure task due to the limitation in patients' exercise performance although it's the common standard to measure the maximum force of muscles. In clinical trials, tissue damage is general in the MVC task process. Instead of measure directly, our study aims to estimate MVC through the bodyweight and rehabilitation phase. Based on the mapping regression between muscle force and sEMG characteristics, we can cut off the certain characteristic to quantize DMA by the predicted MVC from body weight.

MVC is assessed by the subjects' body weight. There is a significant regression relationship between the strength of elbow muscles and body weight [26], and the following equation can be derived.

$$F = C \times W^k \tag{1}$$

F : Muscle force
C : Regression coefficient (flexors = 4.256, extensors = 22.85)
W : Body Weight
k : Slope of regression (flexors = 0.97, extensors = 0.53)

The difference of human species must be considered because the system is applied in China. So that we set up a series of experiments to amend the coefficient in (1).

Furthermore, there are statistical differences and regularity of limb muscle strength between the affected side and the healthy side after acute stroke [27]. Hence, we can assess the MVC of patients after stroke by movement type based on (2).

$$F_{mvc} = C \times C' \times W^k \tag{2}$$

F_{mvc} : Predicted muscle force
C, W, k : Like (1)
C' : Object type coefficient

2) FEATURE EXTRACTION

In this study, the sEMG features preparing for visualization need to be insignificant in computational cost, so that the scene on the screen can provide prompt guidance and tips. Subsequently, it's important to select the most appropriate sEMG characteristic to demonstrate the mapping relationship between force and DMA. Firstly, we employed the threshold process to remove the voltage amplitude determined by individual quiescent conditions [23]. Then, we chose a series of time-dependent sEMG features in low-cost operation to compare the performance of prediction accuracy.

We introduce the Time-Dependent Power Spectrum Descriptors (TD-PSD) [28] and the common sEMG characteristics like mean of absolute value (MAV), root mean square (RMS), and integrated EMG (iEMG) to compare these features from the time domain. On account of the original sEMG signal which needs derivation is readily affected by noise, it is important to normalize the extracted feature values to reduce the impact of noise. At the same time, we use log-scaled-amplitudes to an appropriate power [29]. Given an sEMG sequence $x[j]$, with $j = 1, 2, \ldots N$, we can get the following features related to the DMA:

Root squared zero-order moment ($\bar{m}_0$): The features to describe the strength of muscle contraction, like (3)

$$\bar{m}_0 = \sqrt{\sum_{j=1}^{N} x[j]^2} \tag{3}$$

Root squared second and fourth-order moment: like (4)

$$\begin{cases} \bar{m}_2 = \sqrt{\dfrac{1}{N}\sum_{j=1}^{N} (\Delta x[j])^2} \\ \bar{m}_4 = \sqrt{\dfrac{1}{N}\sum_{j=1}^{N} \left(\Delta^2 x[j]\right)^2} \end{cases} \tag{4}$$

We empirically introduce $\lambda = 0.1$ to normalize $\bar{m}_0$, $\bar{m}_2$ and $\bar{m}_4$ with a power transformation [29] in (5):

$$\begin{cases} m_0 = \dfrac{\bar{m}_0^{\lambda}}{\lambda} \\ m_2 = \dfrac{\bar{m}_2^{\lambda}}{\lambda} \\ m_4 = \dfrac{\bar{m}_4^{\lambda}}{\lambda} \end{cases} \tag{5}$$

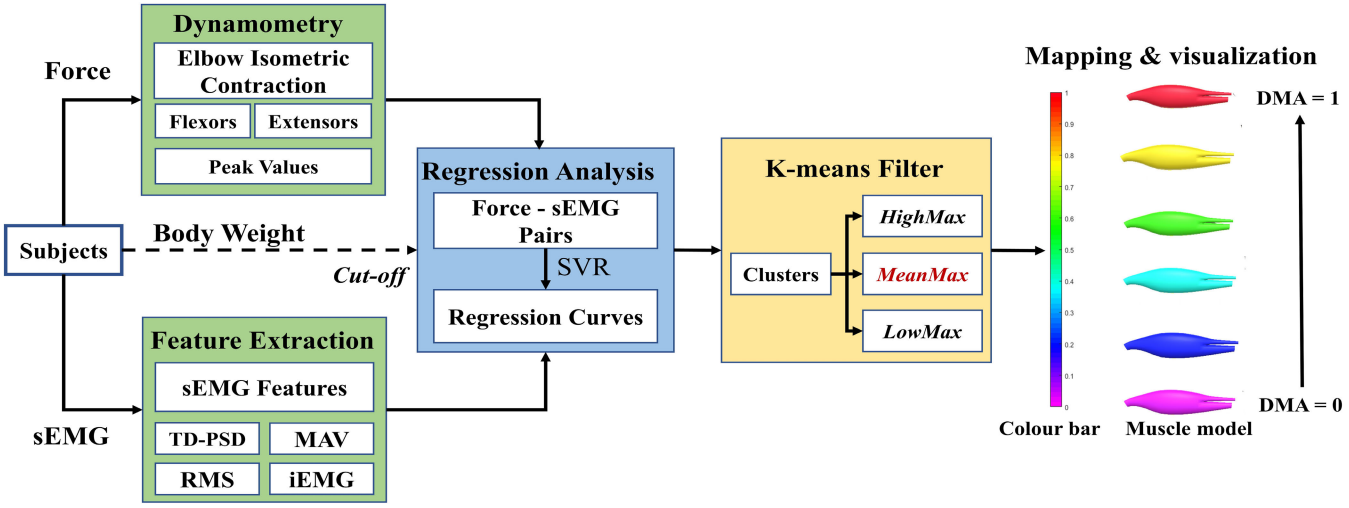

FIGURE 4. Flowchart of the method. Firstly, the force and sEMG data are extracted to feature key-value pairs respectively. Then, force-sEMG pairs are regressed by SVR. The predicted sEMG feature enters into a K-means filter to wipe out the abnormal data. At last, the sEMG after normalization is a value between 0 and 1, which can be mapped to the color bar.

and the final features are shown in (6):

$$\begin{cases} f_1 = \log(m_0) \\ f_2 = \log(m_0 - m_2) \\ f_4 = \log(m_0 - m_4) \end{cases} \tag{6}$$

MAV is the absolute value of the sEMG signals, it is proved to follow a linear relationship with force [30]. The similar indicators are RMS and iEMG in (7)

$$\begin{cases} MAV = \dfrac{1}{N}\sum_{j=1}^{N} |x[j]| \\ RMS = \sqrt{\dfrac{1}{N}\sum_{j=1}^{N} x[j]^2} \\ iEMG = \sum_{j=1}^{N} |x[j]| \end{cases} \tag{7}$$

Participants were required to output the target force. For controlling the variable, we set the sample time 3 seconds both in the control and experimental groups. And under the same mode of exertion, the N in Eq. 7 is a constant parameter depending on sample frequency 1000Hz. The size of window width affects the delay of sEMG processing [31]. We need to choose the appropriate size by taking the error rate and the real-time requirement into account. According to the statistical result in the influence of window length on recognition rate [32], the parameter N is less than 150 and more than 90. And we selected 128 as the window width N.

In the confirmatory experiment, we collected the original sEMG signal and processed it into the aforesaid 6 features, and compare the difference of performance in MVC prediction [33]. For building a mapping relationship between sEMG and the colour of module materials, further processes need to be added [30], [31]. In this paper, we calculate the max of the sEMG feature as the standard of normalization processing, so that the muscle condition can be quantized as a value between 0 and 1. Additionally, MVC is the other

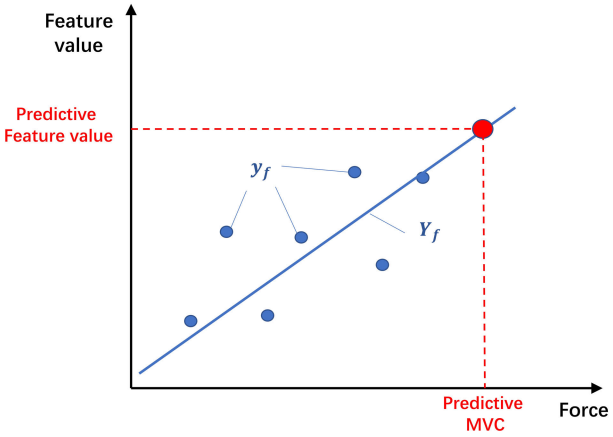

FIGURE 5. The predictive sEMG feature value based on SVR.

efficient standard to normalize the DMA. In the above methods, the main idea is to measure the maximum value of participants firstly [34]. However, getting the MVC is difficult for patients because people must finish many specific movements more than once [35], [36]. Most of the survivors after stroke have postoperative fatigue and limit limb movement so that they cannot finish all the necessary MVC tasks. Furthermore, instead of testing MVC, we can utilize calibration for a particular repetitive motion to determine the normalization factor.

3) REGRESSION ANALYSIS

Support vector regression (SVR) is a regression method to make the total error as small as possible so that we can obtain a fitted curve. In our study, sEMG feature values and the corresponding force values constituted sample points vector $\boldsymbol{y}_f$ (see in Figure 5) in a two-dimensional coordinate. Through the employment of the linear kernel SVR model, the system

can generate a curve $\boldsymbol{Y}_f$ for $\boldsymbol{y}_f$ to cut out the predicted sEMG feature value by the actual MVC. This approach establishes a relationship between easily obtainable weight and the benchmark of DMA normalization.

4) K-MEANS FILTER

In the actual work of visualization of the system, each channel of muscle should process its real-time data separately during DMA visualization for keeping the immersion of participants.

Algorithm 1 Initialization of the Three Clusters

Input: The number of sEMG channel, n **;** The data during the calibration in each channel: *dataset*;
Output: Three clusters: *HighMax*, *MeanMax*, and *LowMax*;

```
/* Traversal of every sEMG channel*/
for i = 0; i < n; i++ do
    /* Initialization of three clusters in each channel*/
    for j = 0; j < dataset.size; j++ do
        HighMax = max (dataset) ;
        MeanMax = mean (dataset) ;
        LowMax = 0;
    end for
end for
return HighMax, MeanMax, LowMax;
```

Algorithm 2 Update the Three Clusters

Input: The number of sEMG channel, n**;** The real-time data in each channel: *dataset*;
Output: Three clusters: *HighMax*, *MeanMax*, and *LowMax*;

```
/* Traversal of every sEMG channel*/
for i = 0; i < n; i++ do
    /* Update three clusters in each channel*/
    for j = 0; j < dataset.size; j++ do
     if (dataset − HighMax) is the minimum then
        HighMax = mean
        {dataset, (dataset − HighMax)} ;
     end if
     if (dataset − MeanMax) is the minimum then
        MeanMax = mean
        {dataset, (dataset − MeanMax)} ;
     end if
     if (dataset − LowMax) is the minimum then
        LowMax = mean
        {dataset, (dataset − LowMax)} ;
     end if
    end for
end for
return HighMax, MeanMax, LowMax;
```

In our study, the K-means clustering method is referred to achieve the function of dynamic normalization in real-time [37]. A calibration through finishing the movement for limited times, aiming to eliminate the individual difference is arranged at the beginning of each treat movement. Then three primary clusters as the standard of dynamic normalization are generated as expected. In the typical K-means algorithm, clusters will be produced when all the data got ready, and the dataset is necessary at the beginning accordingly. We define the clusters differently from the traditional K-means algorithm, based on the small amount of data during calibration assisted by the big data during the whole training time. In other words, three clusters named *HighMax*, *MeanMax*, and *LowMax* are generated by the maximum, mean, and zero processing, and updated according to the minimum among the distances between the new data and three clusters over time as shown in Algorithm 1. We call the cluster updating procedure sampling due to the feature that update interval can be specified as need of users. Benefit from the dynamic clusters, abnormal signal (such as beyond the standard range) will be classified into *HighMax* and *LowMax* to filtered noise, and *MeanMax* is left to be the normalization standard as shown in Algorithm 2. At the end of each task, all channels of muscle store the *MeanMax* into a database to confirm the standard for the next calibration and more diagnosis steps.

5) MAPPING & VISUALIZATION

Clinical therapists cannot understand sEMG easily because of the abstract form in the time and frequency domain. Therefore, the visualization process is indispensable [38]. It is an essential medical function to show the synergistic and antagonistic relationship between different muscle groups and specific DMA. Furthermore, it is crucial and necessary to set up a security alert plugin that can warn of possible harm.

In our project, musculoskeletal models including muscles and bones were all created in Maya 2019 (Autodesk Inc., San Rafael, USA) and imported into Unity as a prefab which can be rendered with different texture maps. The prefab consists of muscles and bones two major parts. On one hand, the muscles part is loaded DMA information over the actual arm tracked by the mark image through the smartphone camera. On the other hand, the bone part leads the body in VEs to move in real-time. As the child component, the muscle part can transform (position and rotation) with the bones part and show the muscle condition (DMA and abnormal activity modes) at the same time. After receiving the sEMG data, the visualization system will drive the material of muscles to change color in a predetermined direction smoothly. Figure 4 shows the color response of the material of muscles after triggered, and finally, achieves the purpose of visualization.

In some cases (compensatory or force overload, etc.), patients will move their arms in an unexpected way which seriously affects the rehabilitation effect of patients and even endangers the health of muscle tissue during the rehabilitation process. The expression ability and emotional control of patients after stroke are reduced to a certain extent. The emotional disclosure of compensation and overload is often complicated and delayed, so the stroke rehabilitation supervision system must be able to detect and display early warning information promptly.

TABLE 2. Particulars of object type coefficient.

Object type	Action type	
	Flexors	Extensors
Predicted	1	1
Stronger	0.721	0.845
Weaker	0.391	0.456

D. PERFORMANCE EVALUATION

$$\begin{cases} \bar{y} = \dfrac{1}{n}\sum_{i=1}^{n} y_i \\ SS_{tot} = \sum_{i} (y_i - \bar{y})^2 \\ SS_{reg} = \sum_{i} (f_i - \bar{y})^2 \\ R^2 = \dfrac{SS_{reg}}{SS_{tot}} \end{cases} \tag{8}$$

In our work, the regression performance in the MVC prediction was evaluated by the R^2, which reflects the relationship between mass and the actual MVC. To study how the sEMG features perform, we introduced the predictive accuracy that representing the ratio of the predicted value to the measured value after normalization.

$$a_{pre} = \frac{v_{mea}}{v_{pre}} \tag{9}$$

Considering the sEMG feature type and the force-sEMG pairs data scale can influence the result, we employ a_{pre} to evaluate the prediction performance. Where the a_{pre} is the predictive accuracy in [0,1], v_{pre} is the feature value corresponding to the predictive MVC, and the v is the measured feature value. A significance level of $P < 0.05$ was used for all the analyses.

$$k = \frac{y_{max} - y_{min}}{x_{max} - x_{min}} \tag{10}$$

After regression by SVR, a linear curve is generated. We use the slope k to measure the sensitivity of different features. Where the y_{max} is the maximum feature value, x_{max} is the MVC value, and the minimum value is the antithetical.

III. RESULTS

A. COEFFICIENT OF MVC PREDICTION

The linear regression in Fig. 6(A) shown that the linear models can predict MVC by body weight in a significant correlation ($R^2 = 0.834$ in biceps and $R^2 = 0.795$ in triceps).

As shown in Figure 6(B), the correction coefficients of elbow flexor and extensor muscles were 0.593 ± 0.006 and 0.434 ± 0.027 respectively. There were significance differences ($P = 0.01 < 0.05$). And the prediction model converts to:

$$MVC = C \times C_{com} \times W^k \tag{11}$$

MVC : Maximum autonomic contraction peak
C : Regression coefficient (flexors = 4.256, extensors = 22.85)
C_{com} : The compensation factor (flexors = 0.598, extensors = 0.434)
W : Body weight
k : Slope of regression (flexors = 0.97, extensors = 0.53)

B. DATA SCALE IMPORTANCE

We chose the small to large data scale from 3 because of the excessively low accuracy and abnormal fluctuation in the result. As shown in Figure 7, the log ($m0$) reached the highest a_{pre} in biceps (0.955) and triceps (0.958) when the data scale is 10. On the medium scale (5 - 8), almost all features had the a_{pre} beyond 0.8. Furtherly, the power spectrum features have rapidly risen in this data scale from 0.8 to 0.95. More specifically, in the data scale 6, the MAV a_{pre} is the highest in both muscles.

C. COMPARISON OF FEATURES

In the feature extraction stage, six features of sEMG are considered to represent the DMA mapping to the force bioinformation. The results for analyzing the a_{pre} of 6 different sEMG features with SVR in two muscles (biceps and triceps) and different data scales (10 pairs and 6 pairs) for 10 subjects are shown in Figure 8. It can be noticed that the a_{pre} of log ($m0$) the feature is the highest ($99.3\% \pm 0.54\%$ in biceps and $98.35\% \pm 2.37\%$ in triceps) with 10 pairs key-value, but the error rates in power spectrum features (log ($m0$), log ($m0 - m2$), and log ($m0 - m4$)) significantly enhance while cutting down the force-sEMG key-value pairs from 10 to 6. The error bar of log(m0) in Figure 8(B) also exhibits the influence of the data scale. Inversely, the MAV has good toughness to adapt to different data scales with a high predictive level. In the small data scale situation of 6 pairs, MAV still has the highest a_{pre} of $89.84\% \pm 5.28\%$ in biceps and $84.26\% \pm 6.44\%$ in triceps. There were significance differences ($P = 0.01 < 0.05$).

As a representative, 6 different features of Subject 5 are normalized (the order of magnitude and units of different indexes were significantly different), and the force-sEMG scatter points are plotted in a 2-dimensional coordinate system to perform regression analysis with SVR. The highest k in both biceps and triceps were all the MVC (0.00256 and 0.00188). During the biceps, the k of six features were 0, 0.00064, 0, 0.00256, 0.00056, and 0 respectively. During the triceps, the k of six features were 0, 0, 0, 0.00188, 0, and 0 respectively. In Figure 9, the a_{pre} of the power spectrum features were around 1, while the k was less than the other three features.

IV. DISCUSSION

In this paper, we introduce an approach to visualize the degree of muscle activities by sEMG. Our work can map the muscle

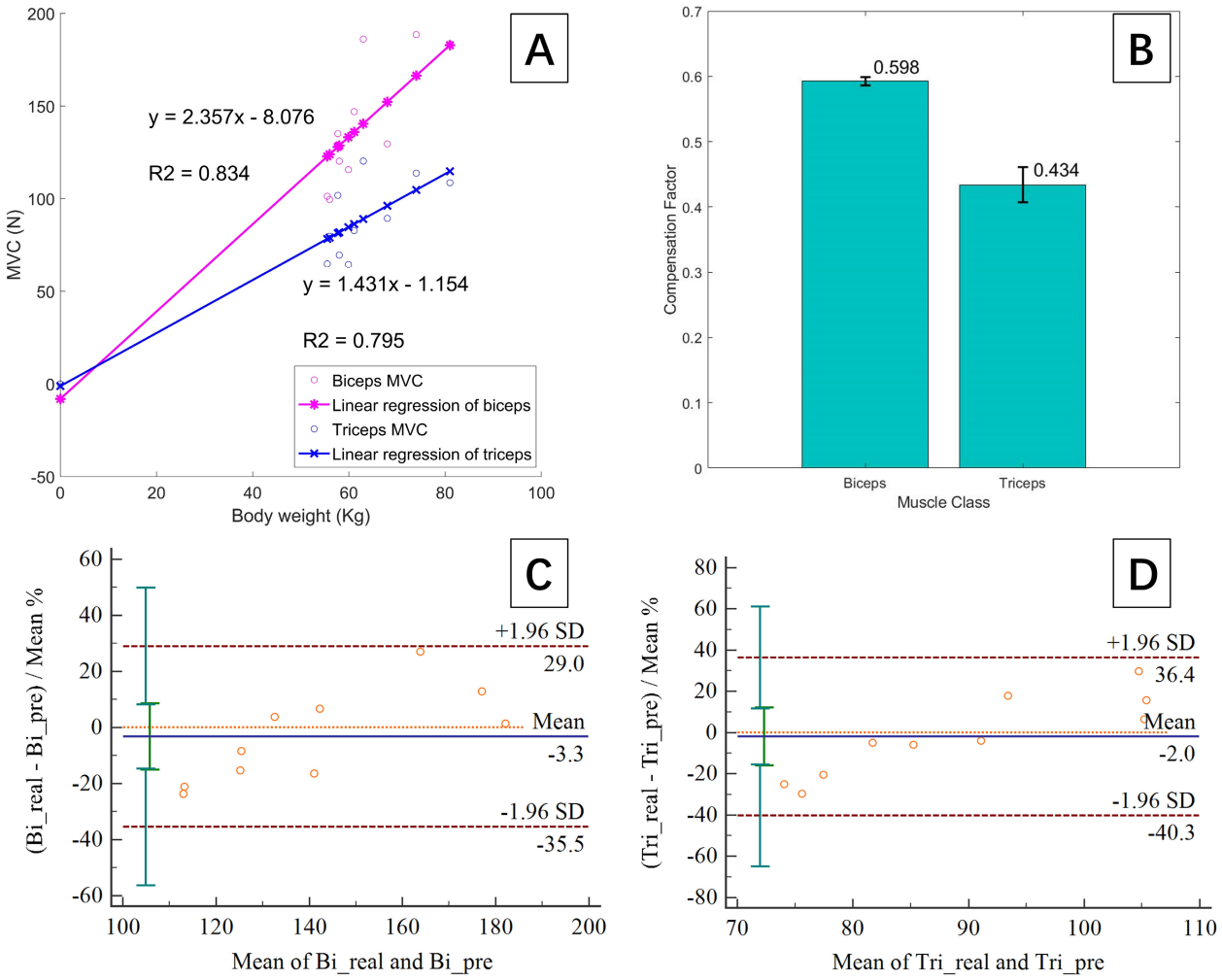

FIGURE 6. **(A) Linear regression of elbow muscle MVC with body weight. (B) The compensation factor for MVC predictions. Standard deviation is shown with error bars. (C) (D) The Bland-Altman plots of the consistency check in biceps and triceps respectively. All sample points are within the CI 95% (−35.5% to 29.0% in biceps and −40.3% to 36.4% in triceps). In addition, compared with the actual measurement, the mean error of the prediction method was 0.545% and 0.758% in biceps and triceps respectively.**

force and the sEMG features, and predict the normalization standard by body weight with the process of filtering the abnormal signal.

The normalization standard which brings the possibility of future clinical trials is deduced through our verify experiment and the previous work [26], [27]. Further, previous studies only provided a method and methodology for MVC prediction, and necessary modifications should be made in combination with regional differences. Through MVC tests on healthy adult men, we deduced and statistically calculated the MVC prediction correction coefficient suitable for Chinese people.

To confirm the appropriate sEMG feature and data scale, we had set up a series of experiments. The experiment for choosing the appropriate sEMG feature and data scales shows that in both biceps and triceps, the major feature accuracy reached 85% when the data scale more than 6. The relationship between the data scale and the predictive accuracy presents a tendency to increase from 5 to 8. Although the highest predictive appears in 10 pairs, we can also focus on the first rising trend that the prediction model crosses the sparse key-value pairs in the initial. The result reminds us to design the calibration economically in the respective action to confirm the standard normalization. Although the accuracy can achieve higher while the data scale growing, the extra workload is difficult and tough for the patients. Besides, considering the results in Figure 6 shows the trend changing by the force data expanding from small to big, the little data scale means the light train tasks. However, the MAV performed in a better adaptation and linear in the force-sEMG regression so that we can normalize the color mapping efficiently. It is evident that in both flexor and extensor muscles, although the three features related to power spectrum have a high accuracy in predicting DMA corresponding to MVC, the distribution cannot reflect the characteristics that grow with the increase of muscle force,

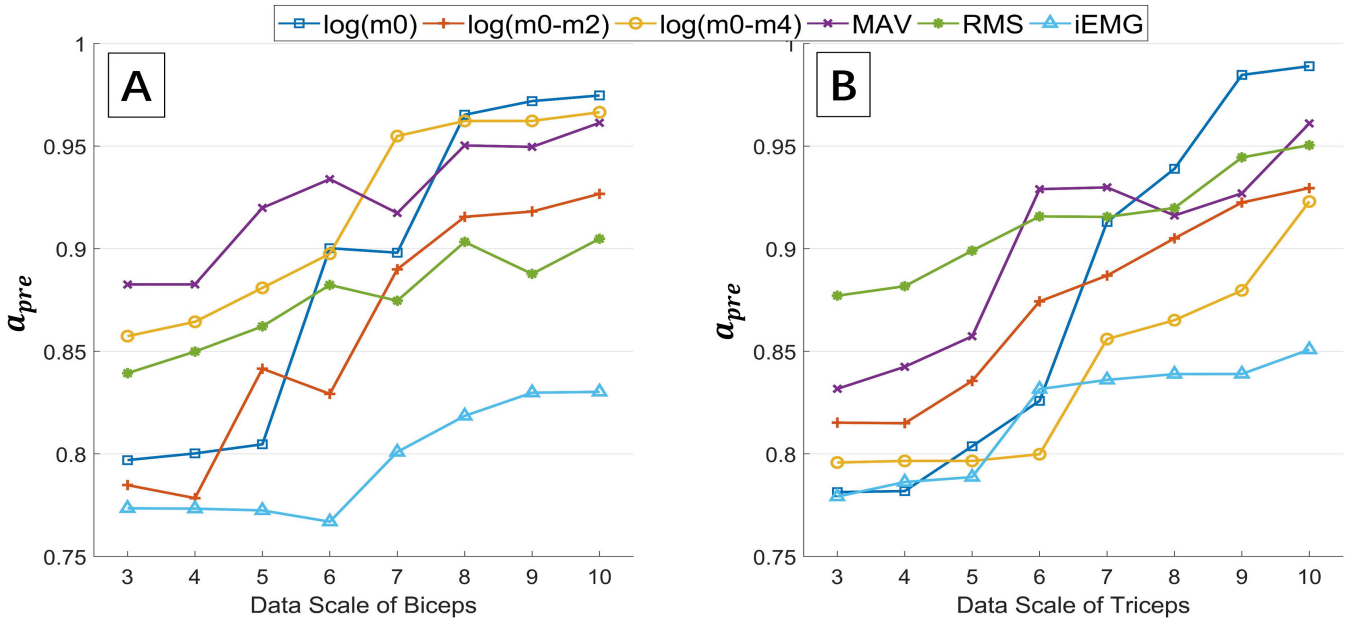

FIGURE 7. The mean accuracy of prediction in 6 sEMG features in different data scales. (A) Biceps. (B) Triceps. There is a significant improvement of accuracy in the data scale between 5 and 8.

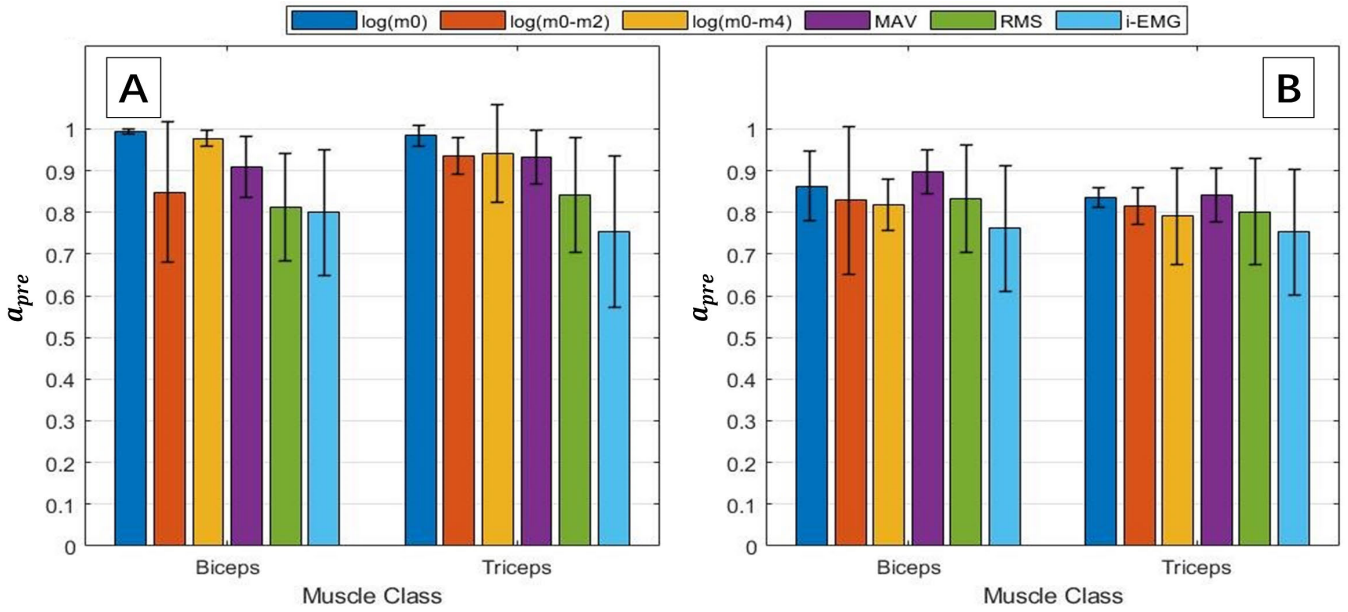

FIGURE 8. The mean accuracy of prediction in 6 sEMG features in different data scales. (A) 10 pairs (B) 6 pairs. Standard deviation is shown with error bars.

which runs counter to the demand to calculate DMA benchmark by few slight force tasks. Concretely, the power spectrum features exceed the predicted value easily (see Figure 9(A)). On the contrary, although the prediction accuracy of MAV, RMS, and iEMG is not as high as features in the power spectrum, the trend of change with force is obvious and on-demand, especially MAV. A linear relationship has a larger slope, which is more suitable for the sEMG feature. Through the experiments of the force-sEMG mapping relationship, we found that MAV is the most appropriate sEMG feature to normalize the DMA of muscles by prediction of MVC.

We also study the efficient approach to resolve the complex condition of visualization. Applying the K-means filter to study the sEMG process, we found that the mapping relationship between muscle force and the degree of muscle activation can be updated in real-time. Our system shows a better real-time capability by using the more efficient algorithm comparing the offline visualization framework [18]. In comparison to previous studies of the scales [9]–[12], the utilization of the sEMG signal can provide the root information with a more implicit meaning of rehabilitation guidance. For visualizing the normalized sEMG signal, a musculoskeletal model built in the virtual environment is superimposed

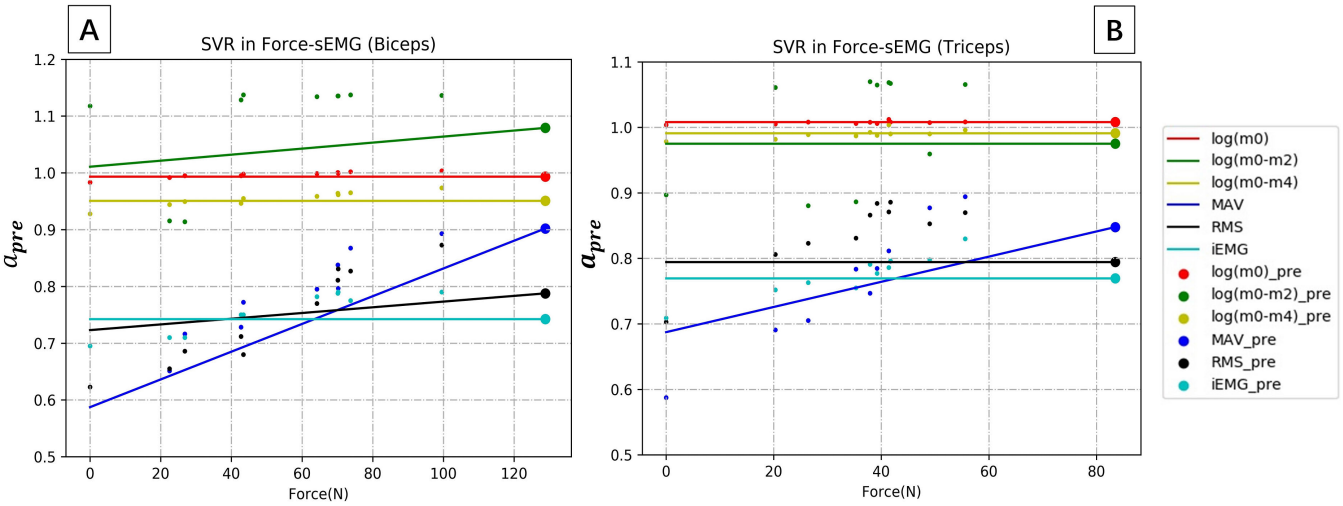

FIGURE 9. Regression curves of 6 sEMG features in Subject 5's (A) biceps and (B) triceps. The points show the normalized predictive feature value.

on arms so that the biological information can be more concretely displayed. Besides, a safety guarantee was in consideration for patients, and we packaged it as a plugin that provides a striking visual effect. We have shown that the supervision system can provide underlying bioinformation of muscle status with portability and low barriers. We noticed that the DMA visualization system conforms to the economic foundation of developing countries, providing a viable option for multi-terminal consultation, training and electronic medical record display under the situation of the cost of EMG equipment is challenging to reduce. As shown in the above parts, the supervision system provides the therapist with a more intuitive approach to observe the rehabilitation condition so that they can consider deeply and arrange a more appropriate rehabilitation process. Some necessary interfaces and components can provide a more complex function, more efficient application scene, and broader research prospect.

Recent research on the visualization of bioinformatics reveals possible compensatory phenomena during stroke rehabilitation training through the movement of the trunk, transforming the therapists' observations into quantified angle information [39], [40]. Similarly, our study considered and quantified the intention of patients to exercise at a deeper level by processing EMG signals. Even if the patient's motor ability is poor, the degree of muscle activation also can be conveyed clearly to the therapist through the display devices. In a recent muscle visualization study [32], the authors focus on how to display DMA of the forearm under different gestures and set a display interface for the supervision and diagnosis of therapists. This approach visualized the DMA by introducing the HSV, but the three-dimensional interaction and biofeedback were neglected because of the planar interface. In our work, the display of DMA is carried by a three-dimensional musculoskeletal model of the human body, so that patients can get biofeedback beneficial to body posture adjustment during the interaction process while the therapists are monitoring the recovery and safety status. In summary, our work focuses on iterating the long-term training results of patients to achieve the self-adapting DMA visualization. Unlike the previous studies, our study aimed to use bioinformation feedback to adequately urge patients to make active exercise status adjustments.

However, in consideration of this research is a pilot study, there is a lot of work that will be carried out: Although low-cost demand comes out in the terminal, the sEMG apparatus is expensive and relies on desktop computers. At the same time, we need more portable wearable sEMG collection devices to reduce the burden of rehabilitation for patients. Furthermore, in the next step, we will evaluate our system through clinical experiments to ensure the effectiveness of our system.

V. CONCLUSION

In this paper, an sEMG visualization system for reducing the difficulty of understanding the condition of muscles has been presented. The system normalizes the DMA through the MAV feature and the K-means cluster algorithm, steering clear of the difficult measurement of MVC for patients after stroke by a calibration step. Then, we design experiments to demonstrate the effect of different sEMG features. The results show that MAV has the best robustness to verified data scale and a relatively higher predictive accuracy. Besides, the alarm module makes full use of the sEMG data to prevent the harmful behaviors of patients. This system is a new supervision method and the future development direction of the rehabilitation medical field.

REFERENCES

[1] G. Alankus and C. Kelleher, "Reducing compensatory motions in motion-based video games for stroke rehabilitation," *Hum.–Comput. Interact.*, vol. 30, nos. 3–4, pp. 232–262, May 2015.

[2] P. Dias, R. Silva, P. Amorim, J. Lains, E. Roque, I. S. F. Pereira, F. Pereira, B. S. Santos, and M. Potel, "Using virtual reality to increase motivation in poststroke rehabilitation," *IEEE Comput. Graph. Appl.*, vol. 39, no. 1, pp. 64–70, Jan. 2019.

[3] S. Albiol-Perez, J.-A. Gil-Gomez, R. Llorens, M. Alcaniz, and C. C. Font, "The role of virtual motor rehabilitation: A quantitative analysis between acute and chronic patients with acquired brain injury," *IEEE J. Biomed. Health Informat.*, vol. 18, no. 1, pp. 391–398, Jan. 2014.

[4] Z. Zhang, Q. Fang, and X. Gu, "Objective assessment of upper-limb mobility for poststroke rehabilitation," *IEEE Trans. Biomed. Eng.*, vol. 63, no. 4, pp. 859–868, Apr. 2016.
[5] J. Schröder *et al.*, "Combining the benefits of tele-rehabilitation and virtual reality-based balance training: A systematic review on feasibility and effectiveness," *Disabil. Rehabil. Assist. Technol.*, vol. 14, no. 1, pp. 2–11, 2019.
[6] E. Tsekleves, I. T. Paraskevopoulos, A. Warland, and C. Kilbride, "Development and preliminary evaluation of a novel low cost VR-based upper limb stroke rehabilitation platform using wii technology," *Disab. Rehabil., Assistive Technol.*, vol. 11, no. 5, pp. 413–422, Jul. 2016.
[7] J. Bai and A. Song, "Development of a novel home based multi-scene upper limb rehabilitation training and evaluation system for post-stroke patients," *IEEE Access*, vol. 7, pp. 9667–9677, 2019.
[8] Y. Li, X. Zhang, Y. Gong, Y. Cheng, X. Gao, and X. Chen, "Motor function evaluation of hemiplegic upper-extremities using data fusion from wearable inertial and surface EMG sensors," *Sensors*, vol. 17, no. 3, p. 582, Mar. 2017.
[9] J. K. Harrison, K. S. McArthur, and T. J. Quinn, "Assessment scales in stroke: Clinimetric and clinical considerations," *Clin. Interv. Aging*, vol. 8, pp. 201–211, Feb. 2013.
[10] L. A. Iacono, C. Wells, and K. Mann-Finnerty, "Standardizing neurological assessments," *J. Neurosci. Nursing*, vol. 46, no. 2, pp. 125–132, 2014.
[11] M. Taylor-Rowan, A. Wilson, J. Dawson, and T. J. Quinn, "Functional assessment for acute stroke trials: Properties, analysis, and application," *Frontiers Neurol.*, vol. 9, pp. 1–10, Mar. 2018.
[12] L. Krumlinde-Sundholm, B. Lindkvist, J. Plantin, and B. Hoare, "Development of the assisting hand assessment for adults following stroke: A rasch-built bimanual performance measure," *Disability Rehabil.*, vol. 41, no. 4, pp. 472–480, Feb. 2019.
[13] L. Y. W. Ho, C. K. Y. Lai, and S. S. M. Ng, "Measuring fatigue following stroke: The Chinese version of the fatigue assessment scale," *Disability Rehabil.*, pp. 1–8, Mar. 2020.
[14] H.-T. Li, J.-J. Huang, C.-W. Pan, H.-I. Chi, and M.-C. Pan, "Inertial sensing based assessment methods to quantify the effectiveness of post-stroke rehabilitation," *Sensors*, vol. 15, no. 7, pp. 16196–16209, Jul. 2015.
[15] B. Oubre, J.-F. Daneault, H.-T. Jung, K. Whritenour, J. G. V. Miranda, J. Park, T. Ryu, Y. Kim, and S. I. Lee, "Estimating upper-limb impairment level in stroke survivors using wearable inertial sensors and a minimally-burdensome motor task," *IEEE Trans. Neural Syst. Rehabil. Eng.*, vol. 28, no. 3, pp. 601–611, Mar. 2020.
[16] H. A. Rahman, K. K. Xiang, Y. C. Fai, E. S. L. Ming, and A. L. Narayanan, "Robotic assessment modules for upper limb stroke assessment: Preliminary study," *J. Med. Imag. Health Informat.*, vol. 6, no. 1, pp. 157–162, Feb. 2016.
[17] H. Chang, J. Zhao, Y. Qiao, H. Yao, X. Wang, J. Li, and J. Liu, "Mobile phone application for self-assessment of acute stroke patients," *Medicine*, vol. 97, no. 26, pp. 4–8, 2018.
[18] N. Pronost, A. Sandholm, and D. Thalmann, "A visualization framework for the analysis of neuromuscular simulations," *Vis. Comput.*, vol. 27, no. 2, pp. 109–119, Feb. 2011.
[19] D. Simonsen, M. B. Popovic, E. G. Spaich, and O. K. Andersen, "Design and test of a microsoft kinect-based system for delivering adaptive visual feedback to stroke patients during training of upper limb movement," *Med. Biol. Eng. Comput.*, vol. 55, no. 11, pp. 1927–1935, Nov. 2017.
[20] L. Pogrzeba, T. Neumann, M. Wacker, and B. Jung, "Analysis and quantification of repetitive motion in long-term rehabilitation," *IEEE J. Biomed. Health Informat.*, vol. 23, no. 3, pp. 1075–1085, May 2019.
[21] M. Stachaczyk, S. F. Atashzar, S. Dupan, I. Vujaklija, and D. Farina, "Multiclass detection and tracking of transient motor activation based on decomposed myoelectric signals," in *Proc. 9th Int. IEEE/EMBS Conf. Neural Eng. (NER)*, Mar. 2019, pp. 1080–1083.
[22] M. C. Tresch, V. C. K. Cheung, and A. d'Avella, "Matrix factorization algorithms for the identification of muscle synergies: Evaluation on simulated and experimental data sets," *J. Neurophysiol.*, vol. 95, no. 4, pp. 2199–2212, Apr. 2006.
[23] K. Ma, Y. Chen, X. Zhang, H. Zheng, S. Yu, S. Cai, and L. Xie, "SEMG-based trunk compensation detection in rehabilitation training," *Frontiers Neurosci.*, vol. 13, pp. 1–12, Nov. 2019.
[24] H. J. Hermens, B. Freriks, R. Merletti, D. Stegeman, J. Blok, G. Rau, C. Disselhorst-Klug, and G. Hägg, "European recommendations for surface ElectroMyoGraphy," *Roessingh Res. Develop.*, vol. 8, no. 2, pp. 13–54, 1999.
[25] P. Konrad, "Skin surface electrodes," in *The ABC of EMG*, 1st ed. Belmont, CA, USA: Noraxon, 2006, pp. 14–16.
[26] S. Jaric, S. Radosavljevic-Jaric, and H. Johansson, "Muscle force and muscle torque in humans require different methods when adjusting for differences in body size," *Eur. J. Appl. Physiol.*, vol. 87, no. 3, pp. 304–307, Jul. 2002.
[27] A. W. Andrews and R. W. Bohannon, "Short-term recovery of limb muscle strength after acute stroke," *Arch. Phys. Med. Rehabil.*, vol. 84, no. 1, pp. 125–130, Jan. 2003.
[28] A. H. Al-Timemy, R. N. Khushaba, G. Bugmann, and J. Escudero, "Improving the performance against force variation of EMG controlled multifunctional upper-limb prostheses for transradial amputees," *IEEE Trans. Neural Syst. Rehabil. Eng.*, vol. 24, no. 6, pp. 650–661, Jun. 2016.
[29] V. Tyagi and C. Wellekens, "On desensitizing the mel-cepstrum to spurious spectral components for robust speech recognition," in *Proc. IEEE Int. Conf. Acoust., Speech, Signal Process.*, vol. 1, 2005, pp. 529–532.
[30] R. Darmakusuma, A. S. Prihatmanto, A. Indrayanto, and T. L. Mengko, "Bicep Brachii's force estimation using MAV method on assistive technology application," in *Proc. 2nd Int. Conf. Instrum., Commun., Inf. Technol., Biomed. Eng. (ICICI-BME)*, Nov. 2011, pp. 288–292.
[31] W. Miao, G. Li, G. Jiang, Y. Fang, Z. Ju, and H. Liu, "Optimal grasp planning of multi-fingered robotic hands: A review," *Appl. Comput. Math.*, vol. 14, no. 3, pp. 228–247, 2015.
[32] Y. Cheng, G. Li, J. Li, Y. Sun, G. Jiang, F. Zeng, H. Zhao, and D. Chen, "Visualization of activated muscle area based on sEMG," *J. Intell. Fuzzy Syst.*, vol. 38, no. 3, pp. 2623–2634, Mar. 2020.
[33] A. Phinyomark, R. N. Khushaba, and E. Scheme, "Feature extraction and selection for myoelectric control based on wearable EMG sensors," *Sensors*, vol. 18, no. 5, p. 1615, May 2018.
[34] A. Phinyomark, R. N. Khushaba, and E. Scheme, "Feature extraction and selection for myoelectric control based on wearable EMG sensors," *Sensors*, vol. 18, no. 5, pp. 1–17, 2018.
[35] A. Phinyomark, P. Phukpattaranont, and C. Limsakul, "Feature reduction and selection for EMG signal classification," *Expert Syst. Appl.*, vol. 39, no. 8, pp. 7420–7431, Jun. 2012.
[36] G. Li, H. Chen, J. Lee, and A. Target, "Information technology—Spring conference a prediction method of muscle force using sEMG," in *Proc. Int. Assoc. Comput. Sci. Inf. Technol. Spring Conf.*, 2009, pp. 501–505.
[37] E. Liberty, R. Sriharsha, and M. Sviridenko, "An algorithm for online K-means clustering," in *Proc. Workshop Algorithm Eng. Exp.*, Jan. 2016, pp. 81–89.
[38] A. Murai, K. Kurosaki, K. Yamane, and Y. Nakamura, "Musculoskeletal-see-through mirror: Computational modeling and algorithm for whole-body muscle activity visualization in real time," *Prog. Biophys. Mol. Biol.*, vol. 103, nos. 2–3, pp. 310–317, Dec. 2010.
[39] S. Cai, X. Wei, E. Su, W. Wu, H. Zheng, and L. Xie, "Online compensation detecting for real-time reduction of compensatory motions during reaching: A pilot study with stroke survivors," *J. NeuroEng. Rehabil.*, vol. 17, no. 1, pp. 1–11, Dec. 2020.
[40] S. Cai, G. Li, E. Su, X. Wei, S. Huang, K. Ma, H. Zheng, and L. Xie, "Real-time detection of compensatory patterns in patients with stroke to reduce compensation during robotic rehabilitation therapy," *IEEE J. Biomed. Health Informat.*, vol. 24, no. 9, pp. 2630–2638, Sep. 2020.

XUYANG WEI received the B.E. degree in mechanical design manufacture and automation from Southwest Jiaotong University, Chengdu, China, in 2017. He is currently pursuing the master's degree with the Shien-Ming Wu School of Intelligent Engineering, South China University of Technology, Guangzhou, China. His research interests include VR rehabilitation and visualization of bioinformation.

YAN CHEN received the B.E. and M.S. degrees in mechatronic engineering from the Hefei University of Technology, Hefei, China, in 2015 and 2018, respectively. He is currently pursuing the Ph.D. degree with the Shien-Ming Wu School of Intelligent Engineering, South China University of Technology, Guangzhou. His research interests include signal processing, machine learning, and upper-limb rehabilitation robotics.

XUEYU JIA received the B.E. degree in software engineering from the South China University of Technology, Guangzhou, China, in 2020, where he is currently pursuing the master's degree with the Shien-Ming Wu School of Intelligent Engineering. His research interests include machine learning and motor imagery.

YITING CHEN is currently pursuing the B.E. degree in process equipment and control engineering with the South China University of Technology, Guangzhou, China. She is preparing to take the master's degree from the Shien-Ming Wu School of Intelligent Engineering, South China University of Technology. Her research interests include visualization of bioinformation and knowledge graph.

LONGHAN XIE (Member, IEEE) received the B.S. and M.S. degrees in mechanical engineering from Zhejiang University, in 2002 and 2005, respectively, and the Ph.D. degree in mechanical and automation engineering from The Chinese University of Hong Kong, in 2010.

From 2010 to 2016, he was an Assistant Professor and an Associate Professor with the School of Mechanical and Automotive Engineering, South China University of Technology, where he has been a Professor with the Shien-Ming Wu School of Intelligent Engineering, since 2017. His research interests include biomedical engineering and robotics. He is a member of ASME.